JOURNAL OF GEOPHYSICAL RESEARCH, VOL. 103, NO. D13, PAGES 16,203–16,219, JULY 20, 1998

Significant reduction in the stratospheric ozone deficit using a three-dimensional model constrained with UARS data

Rashid Khosravi,[1] Guy P. Brasseur,[1] Anne K. Smith,[1] David W. Rusch,[2]
Joe W. Waters,[3] and James M. Russell III[4]

Abstract. We present a near-global analysis of the ozone deficit problem by constraining a fully diurnal, three-dimensional, chemical, radiative, transport model of the middle atmosphere with colocated UARS measurements of ClO, NO_x, H_2O, and CH_4. The domain of the study covers a wide range of altitudes (37.4–49.6 km) and latitudes (62.5°S–27.5°N), for the period of January–February 1992. In this domain, the baseline (no constraints with measurements) model temperatures are mostly warmer than U.K. Meteorological Office (UKMO) observations (by up to 5 K), and the baseline O_3 mixing ratios are underestimated by 10 to 25% relative to HALOE measurements. Also, in this domain the model/data discrepancies in concentrations of the ozone-relevant species are as follows: [H_2O] and [NO_x] are mostly in good agreement, [CH_4] is underestimated by 10-60%, and [ClO] is overestimated by 1.3 to 3 times. We find the following: (1) Constraining the model with UKMO temperatures eliminates about 3-10% of the deficit in the 40-48 km altitude range. (2) Constraining the model with observed NO_x or H_2O (in addition to temperature) has minimal effect on the ozone deficit in most parts of the domain. (3) When the model temperature and ClO profiles are constrained with observations, the deficit is reduced to about 5-15%, bringing the model ozone predictions in the 40 km region to within the uncertainties of HALOE ozone measurements. (4) A 40% reduction in the rate constant of $HO_2 + O \rightarrow OH + O_2$, in addition to constraining T, NO_x, and ClO, eliminates the deficit in portions of the 40 km region and in the upper stratosphere, but it results in 5-10% excess ozone near the equatorial stratopause. (5) When the model methane profile is constrained with HALOE observations and a 6% $HCl + O_2$ channel for the $ClO + OH$ reaction is included in the chemistry, the model ClO abundance agrees well with MLS measurements in most parts of the domain. Further improvement in the ClO abundance can be obtained by decreasing [OH] through reducing the rate constant of the $HO_2 + O \rightarrow OH + O_2$ reaction.

1. Introduction

Over the past 20 years, many models of the middle atmosphere have been developed to help predict possible impacts of natural and human perturbations (e.g., release of chlorofluorocarbons (CFCs)) on the ozone layer. A common characteristic of these models has been underestimation of the abundance of ozone compared to observations [*Solomon et al.*, 1983; *Crutzen and Schmailzl*, 1983; *Brasseur et al.*, 1985; *Eluszkiewicz and Allen*, 1993]. This model/observation discrepancy, which has come to be known as the "ozone deficit problem," is illustrated in Figure 1, which shows that the deficit at 44 km may be as large as about 45% (at 60° in both hemispheres). In the mesosphere, earlier studies have reported even larger deficits [*Rusch and Eckman*, 1985; *Clancy et al.*, 1987]. Over the last 10 years, the model/data discrepancy has been reduced to 10-30% in the stratosphere [*World Meteorological Organization (WMO)*, 1995], largely because of improvements in the absorption cross section and reaction rate data [*Natarajan and Callis*, 1989]. However, it is important to note that the remaining deficit may not be fully explained by the uncertainties in the input reaction rate coefficients [*Natarajan et al.*, 1986], that it is larger than the uncertainties of ozone measurements, and that the deficit exists with respect to independent observations of ozone. Therefore, because ozone is a key "driver" of the chemistry and dynamics in the stratosphere and in order to confidently predict the ozone response due to various phenomena, it is important to reconcile the remaining discrepancy.

Since ozone is in photochemical equilibrium (PE) in the middle to upper stratosphere outside the polar regions, zero- or one-dimensional models have been commonly used to analyze the deficit problem. However, it is important to note that although O_3 itself may be in PE, chemical families such as NO_x that destroy ozone are not and that these families are therefore subject to transport. Since model algorithms employ family partitioning to calculate the profiles of their ozone-destroying members and since the source gases for these members (e.g., N_2O) are also subject to transport, these indirect dynamical effects on the ozone budget should be accounted for. Including these dynamical effects in the calculation of the (baseline) ozone deficit by using a three-dimensional (3-D) model distinguishes the present study from

[1]National Center for Atmospheric Research, Boulder, Colorado
[2]Laboratory for Atmospheric and Space Physics, University of Colorado, Boulder.
[3]Jet Propulsion Laboratory, California Institue of Technology, Pasadena.
[4]Department of Physics, Hampton University, Hampton, Virginia.

Paper number 98JD01084.
0148-0227/98/98JD-01084$09.00

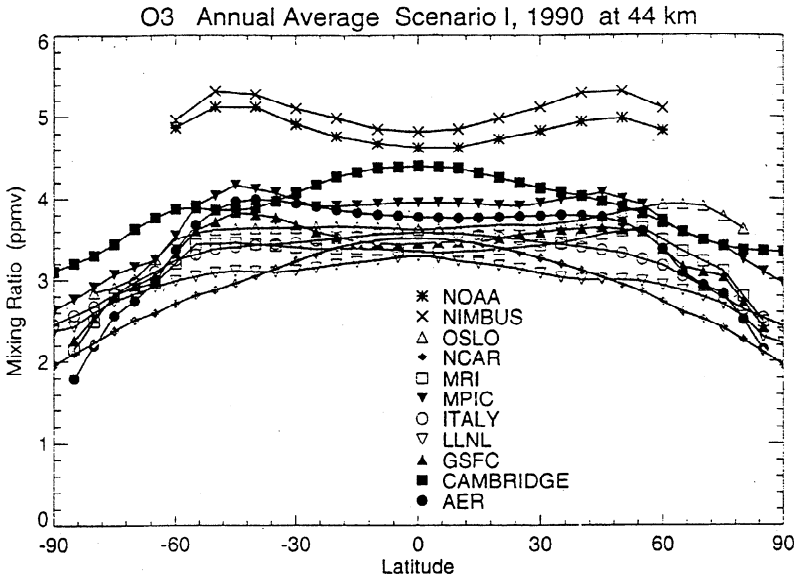

Figure 1. Comparison of the model-calculated ozone concentrations at 44 km (2 mbar) for 1990 with observations (source: WMO [1995] Ozone Report # 37). The observations are the 1989 and 1990 averages from the NOAA 11 solar backscattered ultraviolet (SBUV/2) and the Nimbus 7 SBUV as compiled by *Chandra et al.* [1993]. The mixing ratios are annual averages.

previous investigations. In addition, we constrain our model with simultaneous and colocated measurements of several important ozone-related species (e.g., NO_x and ClO) over a broad range of latitudes thus revealing the near-global behavior of the deficit problem, in contrast to many previous analyses that were performed at one or two latitudes. (Other differentiating aspects of the approach in this study are discussed in section 1.2.)

This paper is organized as follows. In section 1.1, a brief review of the previous studies is presented, followed in section 1.2 by a description of our approach. In sections 2 and 3, we describe the model and the data used in this study, respectively, and in section 4 we present the results. Summary and conclusions are given in section 5.

1.1. Previous Studies

One of the causes investigated for the ozone deficit problem in the past is the uncertainty in the rate coefficients of the reactions involved in loss and production of ozone. *Rusch and Eckman* [1985], for example, found that at 40°N their 1-D model ozone deficit varied with altitude from 30% to 100% relative to Solar Mesosphere Explorer (SME) measurements, maximizing at about 52 km and 65 km in spring and winter, respectively. They found that their model ozone abundance came into near agreement with the SME data when the production rate of OH by $HO_2 + O \rightarrow OH + O_2$ was reduced and the production rate of O_3 by $O + O_2 + M \rightarrow O_3 + M$ was increased to their respective lower and upper limits. *Froidevaux* et al. [1985] also studied the sensitivity of ozone to uncertainties in various rate coefficients. Their 1-D model ozone deficit was as high as 60%, while their model-calculated profiles of HO_x, ClO_x, and NO_x agreed with observed data to within the observational uncertainties (up to 30%). It was concluded that no large adjustment in any one or two rate coefficients would resolve the ozone deficit in the upper stratosphere and that while a combination of many smaller adjustments could significantly reduce the deficit, this was not a satisfactory solution.

Another approach in studying the deficit problem has been to test a model's photochemistry by constraining the model with observed concentrations of the key species and then comparing the resulting ozone distribution with measured profiles. For example, *Jackman et al.* [1986] constrained their 2-D model with H_2O, NO_2, HNO_3, and O_3 measurements by the limb infrared monitor of stratosphere (LIMS) and with CH_4 data acquired by the stratospheric and mesospheric sounder (SAMS). They found that the diurnally averaged ozone loss rate was about 40-60% higher than the production rate in the low-latitude upper stratosphere. However, because the uncertainty in the ozone loss to production ratio was about a factor of 2, it could not be concluded that the model photochemistry [*DeMore et al.*, 1983] was necessarily incomplete. *Froidevaux et al.* [1989] reached a similar conclusion by constraining their photochemical (0-D) model with H_2O, NO_2, and temperature data from LIMS. They found systematic ozone deficit relative to the LIMS data, varying from about 25% at 40 km to about 70% at 65 km. They concluded that since the uncertainties in the model mixing ratios (due to cumulative errors in the input parameters) overlapped the measurement uncertainties, there may not have been any missing chemistry in the model.

The conclusions of *Allen and Delitsky* [1991], however, were different. They initialized their one-dimensional model with the atmospheric and trace molecule spectroscopy (ATMOS) measurements of O_3, NO_x, N_2O, NO_y, HCl, and $ClONO_2$. The ozone abundance calculated by their model was systematically lower than the ATMOS measurements by as much as 45% in the stratosphere and 70% in the mesosphere when the ATMOS measurement uncertainties were accounted for. The deficit reduced to about 10% when the O_2 cross sections in the Schumann-Runge bands and Herzberg continuum were increased by 40%. However, because a similarly adjusted model did not reproduce the O_3 observations by SME in the mesosphere, they concluded that some aspects of the model photochemistry may need modification. A similar conclusion was reached by

Eluszkiewicz and Allen [1993], who constrained their 0-D model with LIMS measurements of temperature, O_3, H_2O, and NO_2. They also constrained their model with a precomputed ClO profile, which was adjusted to lower values since the 2-D model that computed the ClO profile generated CH_4 mixing ratios that were smaller than the SAMS measurements by up to 5 times. The resulting ozone deficit varied from 4 to 12% in the upper stratosphere and from 4 to 20% in the lower mesosphere. They concluded that this remaining deficit points to an incomplete understanding of the ozone photochemistry in the stratosphere and mesosphere.

In contrast to the above studies, *Crutzen et al.* [1995] found ozone surplus, instead of deficit, when they constrained their 0-D model with Halogen Occultation Experiment (HALOE) measurements of O_3, HCl, H_2O, CH_4, and NO_x. They concluded that this was due to insufficient ozone destruction above 40 km in the model and that therefore no new mechanism for ozone production seemed necessary. However, when the reaction rate constants and the constraining HALOE measurements were chosen to lie near their limits of uncertainties, the surplus turned into deficit. Their results will be discussed further in section 4.1.

New mechanisms for production of ozone, in addition to the conventional *Chapman* [1930] mechanism, have also been investigated as a possible solution to the deficit problem. In particular, *Allen* [1986] suggested that ozone could also be produced by collisional relaxation of highly vibrationally excited molecular oxygen (O_2 where $v \geq 26$): O_2 ($v \geq 26$) + $O_2 \rightarrow O_3 + O$. This reaction was later supported by laboratory investigations [*Slanger et al., 1998; Price et al.,* 1993; *Rogaski et al.,* 1993; *Miller et al.,* 1994]. Moreover, *Miller et al.* [1994] also found that including this additional source of ozone in their 2-D model could account for the ozone deficit at 43 km (but not at higher altitudes). However, more recently, *Latimer et al.* [1996] concluded that the rate coefficient for the above relaxation reaction, calculated based on the principle of detailed balance, is much smaller than that obtained from the laboratory studies. It appears therefore that this new mechanism of ozone production requires further investigation.

1.2. Approach

The method used in this study to analyze the ozone deficit problem is also to constrain a model with observed profiles of temperature and the key ozone-destroying radicals (NO_x and ClO). However, our approach differs from those of the previous studies in the following four ways: (1) We do not constrain our model with measurements of ozone itself, so that the calculated O_3 profiles in our study are based entirely on our knowledge of stratospheric ozone photochemistry as described by *DeMore et al.* [1994]. (2) Since analysis of the deficit problem through comparison of ozone production and loss (P/L) terms can be inconclusive, due to their high sensitivity to uncertainties in the input parameters [*Dessler et al., 1996*], we compare model calculations of NO_x, ClO, and O_3 abundances with measurements directly. (3) We constrain the model with T, NO_x, and ClO individually to isolate and quantify their effects on the ozone abundance. (4) The domain of our study (section 3.3) is broad in latitude (and altitude), which allows analysis of the ozone deficit problem on a near-global scale. In addition, because the model is fully diurnal, it allows accurate comparison of model profiles of NO and NO_2 with the observed distributions (HALOE, sunset). This, in turn, allows constraining the model (section 3) accurately with NO and NO_2 measurements. A similar advantage holds for comparing and constraining the model ClO with MLS observations.

2. Model Description

The model used in this study is a modified version of that described in detail by *Rose* [1983] and *Rose and Brasseur* [1989]. The modifications are described by *Smith* [1995]. It is a global, 3-D, dynamical, chemical, radiative model which extends from 10 to 80 km in altitude. The resolutions in altitude, latitude, and longitude are about 3 km, 5°, and 11.25°, respectively. A semi-Lagrangian scheme for transport [*Smolarkiewicz and Rasch,* 1991] and the Euler method for computing the concentrations of the chemical species are used. Photolysis rates are interpolated in altitude, albedo, ozone column amount, and solar zenith angle, from a lookup table. The table is constructed by a radiative transfer code which is based on the order-of-scattering method [*Goody and Yung,* 1989], using 6 orders of scattering. Photolysis of O_2 in the Schumann-Runge bands is computed by the parameterization of *Kockarts* [1994]. The reaction rate constants and absorption cross sections are taken from *DeMore et al.* [1994] (hereafter called JPL94), and the solar irradiances are obtained from the measurements of Solar Stellar Irradiance Comparison Experiment (SOLSTICE, onboard UARS). In a recent evaluation, the model's mixing ratios and photolysis rates have compared well against benchmarks from NASA (chemistry) and the University of California, Irvine (photolysis rates).

2.1. Dynamics

The model solves the fundamental equations in flux form [*Rose and Brasseur,* 1989; *Smith,* 1992] to derive the temperature (T), geopotential (Φ), and wind fields (u, v, w). The diabatic forcing includes heating by O_3 and cooling by CO_2, O_3, and H_2O. The heating rates are computed by using the parameterization of *Schoeberl and Strobel* [1978], which includes contributions from all the major absorption bands of ozone (Schumann-Runge continuum and bands, Herzberg continuum, Hartley band, Huggins bands, and the Chappuis bands). The infrared cooling rates are computed by the algorithm of *Zhu et al.* [1992] and *Zhu* 1994] which solves the flux form of the radiative transfer equation via Curtis matrix interpolation.

2.2. Boundary Conditions

Tropospheric forcing is simulated by applying climatological zonal mean fields of u, v, T, and Φ to a level below the lower boundary (near the 350 mbar surface). Wave forcing in the geopotential field is simulated by applying observed geopotential waves (National Centers for Environmental Prediction (NCEP) climatology for January). All these fields are interpolated in time. The other boundary conditions are as follows: The vertical wind is set to zero above the top boundary (at 81.5 km), and the horizontal wind components are set to zero at the poles.

2.3. Chemistry

Gas-phase concentrations of 27 long-lived species and 14 short-lived species are calculated at each time step by the backward Euler method, iterated 4 times. The long-lived species include odd oxygen ($O_x = O + O_3$), odd nitrogen ($NO_x = NO + NO_2$), odd chlorine ($ClO_x = ClO + Cl$), and odd bromine ($BrO_x = Br + BrO + BrCl$). In addition, two larger families of chlorine and nitrogen species are adopted. These are $Cl_x = ClO_x + OClO + 2Cl_2O_2 + HCl$

+ $ClONO_2$ + HOCl + $2Cl_2$ + $ClNO_2$ and $NO_y = NO_x + HNO_3 + 2N_2O_5 + HO_2NO_2 + ClONO_2 + BrONO_2 + NO_3 + N$. The Cl_x concentration is prescribed to ~ 3.2 ppbv, which is the appropriate value for the early 1990s [*WMO*, 1995], since the timescale for significant change in the total chlorine burden of the stratosphere is about 1 year (0.13 ppbv per year from 1985 to 1992 [*WMO*, 1995]).

2.4. Initialization

The initial fields of u, v, and T are generated by using the procedure of *Kurihara and Tuleya* [1978] in a zonally symmetric, dynamics-only version of the model that relaxes to climatological fields (COSPAR International Reference Atmosphere). The initial fields therefore not only agree with the climatological profiles, but they also obey the model equations, including gravity wave drag and radiative forcing. Mixing ratios of the chemical species are initialized by the output of the 2-D model of *Brasseur et al.* [1990]. This procedure provides an internal consistency between the mixing ratio fields of the species.

3. Data Description

The data used in this study consist of U.K. Meteorological Office (UKMO) temperatures, ClO from the Microwave Limb Sounder (MLS), and O_3, NO, NO_2, CH_4, and H_2O from the Halogen Occultation Experiment (HALOE). Both instruments are onboard the Upper Atmosphere Research Satellite (UARS), which was launched on September 12, 1991 [*Reber*, 1993], and both have been providing high-quality data almost continuously since launch. The MLS data employed are version 3, and the HALOE data used are version 18 sunset. We note that the differences between HALOE sunset and sunrise measurements of ozone are nearly zero in the lower to middle stratosphere, increasing to about 5% (root-mean-square) near the stratopause where the average sunset ozone values are higher than the average sunrise values [*Brühl et al.*, 1996]. Therefore, since the domain of our study is in the upper stratosphere (section 3.3), by using the larger (sunset) ozone profiles our analysis covers the worse case ozone deficit scenario that would result from using HALOE ozone data for both modes.

Except for O_3, the above data are used to constrain the model in order to help isolate the causes of the deficit problem. For each species of interest, this is done by first calculating the zonal averages of the measurements (sections 3.1 and 3.2), which are then interpolated to the model altitude/latitude grids. The resulting map is then divided by the zonal averages of the mixing ratios of that species calculated by the model in an initial run. (The model zonal averages are obtained in the same way as those for the measurements.) For example, for NO_2, this procedure yields the ratio H/M of the sunset zonal mean of the mixing ratios measured by HALOE (H) to the sunset zonal mean of the mixing ratios calculated by the model (M) at all model altitude/latitude grid points in every time step. In a second, identical model run in every time step the model NO_2 mixing ratios at all sunset and daytime grid points are multiplied by H/M, thus constraining the model with the HALOE measurements of NO_2.

The same procedure is used for constraining the model with NO, H_2O, CH_4, and ClO, except that for ClO, daytime zonal averaging is used instead of sunset zonal averaging (section 3.2), since the daytime mixing ratio of ClO is approximately constant. In the case of temperature, because the observed fields are available at every model longitude and because diurnal variations are negligible, the above procedure is not necessary, and the temperature data for any particular day are used directly in the model in every time step.

We note that the data-to-model ratios discussed above represent an entire period during the simulation and thus cannot be updated for each model day, because of limitations imposed by the geometry of the measurements. This can be seen as follows: In the case of HALOE data, because each latitude is covered on a different day (section 3.1), the data-to-model ratio is obtained by dividing the HALOE data by the model profile on the corresponding days. For example, on January 6, 1992, HALOE provided 15 measurements of the vertical profile of NO at 62.5±1°S (approximately), each at a different (sunset) longitude. We take the average of these 15 measurements and regard it as the HALOE NO data at 62.5°S. We then take the ratio of this profile to the sunset zonal mean of the model profile of NO at 62.5°S that was calculated on January 6, 1992. This ratio is then used to constrain the model NO at 62.5°S in every model day. We cannot update this ratio for each new model day, because from January 7 through February 13, 1992, HALOE measured NO at latitudes other than 62.5°S.

When using MLS measurements, the data-to-model ratios of ClO cannot be updated daily, since the measurement geometry generally allows coverage of approximately two local times per day at any latitude. Thus, to obtain the daytime zonal mean of the ClO mixing ratios measured by MLS at 62.5°S, for example, we must average the daytime ClO data over the entire UARS yaw period in order to cover a large sample of local times. The model daytime zonal mean of ClO at 62.5°S is obtained in the same manner; that is, we average the model daytime ClO mixing ratios over the entire period. The ratios of the so-obtained MLS data and the model calculations are then used in every day of the simulation to constrain the model at 62.5°S with the measurements. Therefore, in this case also, the nature of the measurement geometry does not allow daily updating of the data-to-model ratios at each latitude.

It should also be noted that the UKMO temperatures used in this study have uncertainties associated with them, as do any other data set of temperatures. An alternative global set of temperature data that would have been suitable for use in our study are the NCEP temperatures, which, like UKMO, are derived based on an analysis technique incorporating radiosond and satellite measurements. A recent study comparing UKMO and NCEP temperatures [*Manney et al.*, 1996] has concluded that in general, "... there is broad agreement between the two analysis data sets. Both sets of analyses provide a good meteorological framework to describe the overall characteristics and evolution of the stratospheric circulation ... ." Therefore, because of this broad agreement, we would have obtained similar results regarding the effect of temperature on the ozone deficit had we used NCEP temperatures.

3.1. Processing of HALOE Data and Model Output

HALOE employs the solar occultation technique [*Russell et al.*, 1993] to retrieve vertical profiles of O_3, HCl, HF, CH_4, H_2O, NO, NO_2, aerosol extinction, and temperature. Measurements are made in either sunset or sunrise mode, and the geometry of solar occultation allows generally 15 measurements in each mode per day. The 15 measurements are obtained at nearly the same latitude. This means that the vertical profiles of each species measured during any one day correspond to a particular latitude

(but different longitudes). Therefore an altitude versus latitude map of a species mixing ratio measured by HALOE represents a period of many days, the vertical profile at each latitude being the zonal average of the profiles obtained on the day corresponding to that latitude. After processing the HALOE data in this manner, they are interpolated to the model's altitude/latitude grids to allow a one-to-one comparison with model profiles at each model grid point.

The model profiles are processed in a similar manner to compute the ratios of HALOE data to model mixing ratios. First, the sunset zonal mean of a species mixing ratio is obtained for all days in the simulation. From these daily mixing ratio sets, the altitude profile at any latitude is taken for the same day on which HALOE obtained measurements for that latitude. This eliminates possible errors that could be introduced when a model profile corresponding to a single day is compared with HALOE measurements representing a period of 1 month or longer (38 days in this study from January 6 to February 13, 1992).

3.2. Processing of MLS and Model ClO

MLS employs the limb scanning technique to retrieve vertical profiles of temperature and O_3, H_2O, and ClO mixing ratios. The instrument is described by *Barath et al.* [1993], and the microwave limb sounding technique is described by *Waters* [1993]. The geometry of this technique allows daily measurements at all latitudes viewable during a particular UARS yaw period (e.g., 80°S–32°N from January 15 to February 13, 1992). However, the range of local times covered at each latitude is limited during any one day, so that to obtain statistically accurate zonal means, data sets over the entire yaw period must be used.

All ClO data are screened for the appropriate quality parameters and multiplied by 0.92, as recommended by *Waters et al.* [1996]. In addition, all negative ClO mixing ratios in the MLS data sets (caused by instrument noise, which has both positive and negative effects) are included in order not to introduce positive bias in the zonal means [*Waters et al.*, 1996]. However, those altitudes and/or latitudes at which the resulting zonal average is negative are excluded from the data set with which the model is constrained.

3.3. Spatial Domain of the Study

The altitude/latitude exclusion just described determines the lowest altitude (37.4 km) and the highest latitude (27.5°N) at which ClO and all other species are constrained in the model. The upper bound in altitude (49.6 km) and the lower bound in latitude (62.5°S) are determined by the constraints imposed by HALOE coverage during the period of January–February 1992. These constraints are the highest altitude at which there is no missing NO_2 data across all covered latitudes and the lowest latitude of observation, respectively.

4. Results and Discussion

In Plate 1, the ozone profile calculated by the baseline model, which is defined as the version of the model that is not constrained with any measurements and in which no modification is done to the standard chemistry (JPL94), is compared with HALOE measurements. It is seen that the model reproduces the altitude/latitude dependence of the observed ozone profile reasonably well and that below 35 km the model/data discrepancy is within the 12% root-sum-square (rss) uncertainty of the HALOE ozone measurements [*Brühl et al.*, 1996]. The deficit increases with altitude to local maxima (typically 20%) in the 40-45 km region, then decreases to a local minimum near the stratopause.

In the middle to upper stratosphere, ozone loss is controlled by the catalytic mechanisms involving NO_x, ClO, and OH [*Brasseur and Solomon*, 1986] and by the Chapman reaction, $O + O_3 \rightarrow 2O_2$. Therefore, since chlorine, nitrogen, and ozone chemistry is temperature-sensitive, we first examine the model temperature profile, shown in Plate 2 for the domain of this study (section 3.3). It is seen that above 40 km (except poleward of 25°S) the model stratosphere is warmer than that observed by as much as 5 K but is cooler below 40 km. This discrepancy in the temperature profile affects the ozone budget significantly, on the same order as the 8–9% rss measurement uncertainties of ozone in this region. As Plate 3c shows, when the model temperature is constrained to the observed profile, the ozone deficit decreases as much as 8–10% in the tropical upper stratosphere. This is mainly due to the large activation energy of the above Chapman reaction, which plays an important role in the loss rate of O_3. For example, the loss rate of ozone by this reaction ($\propto \exp(-2060/T)$ (JPL94)) decreases by 2.9% for a 1 K reduction in temperature from 265 K to 264 K. Thus model/observation discrepancy in temperature is identified as a significant cause of the ozone deficit problem, and hence, in the subsequent analyses, temperature is constrained in order to isolate the other causes of this problem.

Since catalysis of $O+O_3$ by NO_x provides the largest loss rate of ozone in the middle stratosphere, we first investigate possible discrepancies in the calculated NO and NO_2 relative to HALOE measurements. The comparison is shown in Figures 2 and 3, respectively. Figures 2c and 3c show that the model profiles of these radicals are in good agreement with the observed profiles in most of the domain of the study. It is therefore expected that constraining the model NO and NO_2 would have little impact on the ozone deficit, except at the lowest altitudes of the domain in the southern hemisphere where the higher observed NO_x in that region would increase the deficit. These effects can be seen by comparing Plate 4a (T and NO_x constrained) with Plate 3b (only T constrained). Therefore, in our model, NO_x is not a significant cause of the ozone deficit problem in most parts of the domain.

The situation is quite different with ClO. As shown in Plate 5, the model substantially overestimates the abundance of ClO in the middle to upper stratosphere relative to MLS measurements. Near the 40 km region, where ozone loss is dominated by the ClO_x family, the model ClO mixing ratios are 1.7 to 2 times the observed values (Plate 5c). This overestimation, which is believed to be a characteristic of the standard chemistry, is consistent with the findings of other investigators [e.g., *Dessler et al.*, 1996; *Jackman et al.*, 1996; *Michelsen et al.*, 1996]. In section 4.1, we investigate possible solutions for this problem.

It is therefore expected that when the model ClO profiles are constrained to those observed by MLS, the calculated ozone abundance would increase substantially, resulting in a corresponding decrease in the deficit. This can be seen by comparing Plate 4b (T and ClO constrained) with Plate 3b (only T constrained). Plate 4b also shows that when the model temperature and [ClO] agree with observations, the deficit near the stratopause and in the 40 km region (the so-called "40 km ozone problem") is reduced to within the 8–9% uncertainties of the O_3 measurements [*Brühl et al.*, 1996].

The combined effect of bringing the model profiles of T, NO_x, and ClO into agreement with observations is presented in Plate 4c.

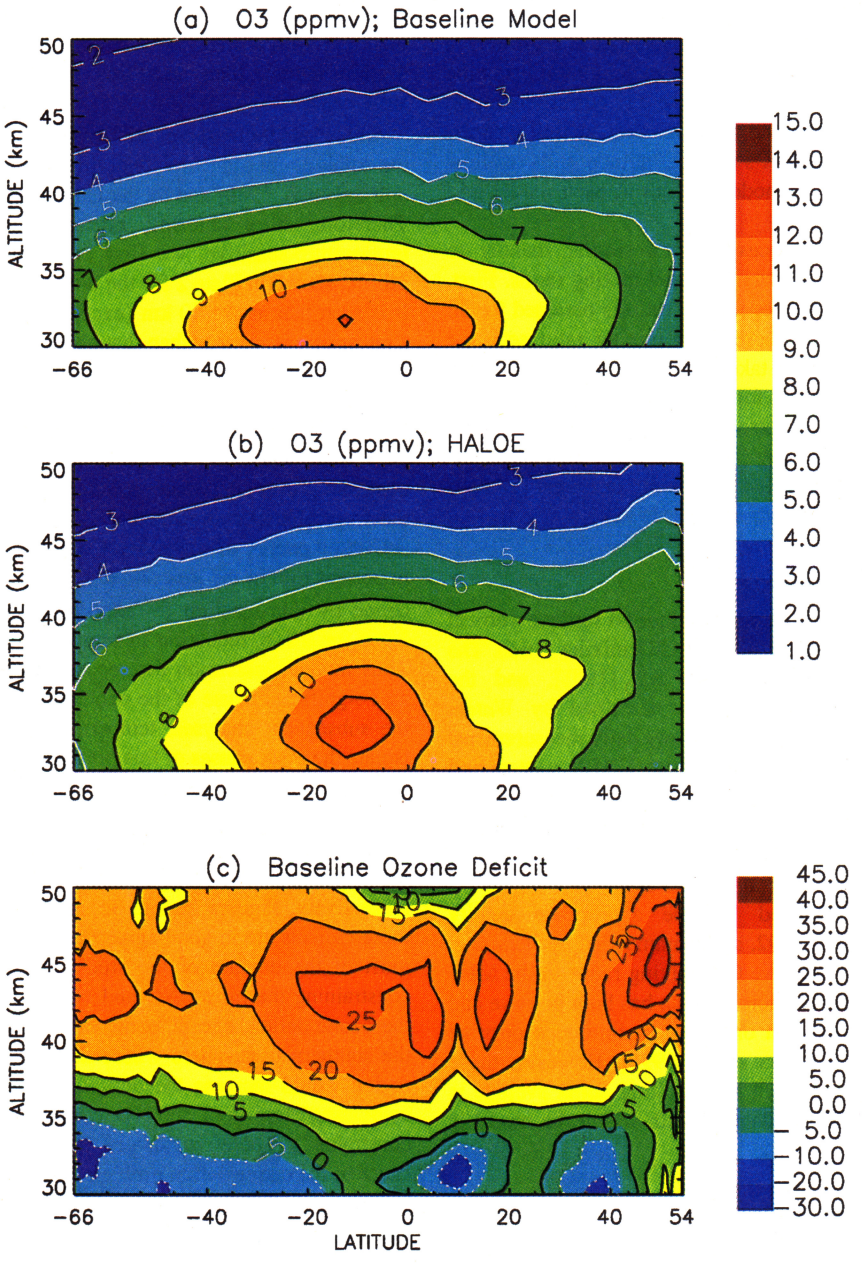

Plate 1. Comparison of (a) the baseline model (nothing constrained) ozone profile with (b) Halogen Occultation Experiment (HALOE) observations. Both profiles show sunset zonal means and are processed for the period of January 6 to February 13, 1992 (section 3.1). (c) The baseline model ozone deficit profile as 100x(HALOE-model)/HALOE. The dotted contours represent overestimation by the model.

Comparison of Plates 4c and 4b shows that the excess ozone near the tropical stratopause and poleward of 40°S in the 40 km region disappears when the model NO_x also agrees with the measured profiles. Also, comparison of Plates 4c and 3a shows that relative to the baseline model a significant reduction in the ozone deficit can be obtained by correcting the temperature and ClO profiles.

To deal with the remaining 10–15% ozone deficit in the upper stratosphere, we consider next the role of the HO_x family in the ozone budget. Figure 4 shows the difference between the model predictions and HALOE observations of H_2O. It is seen that the model underestimates the water vapor abundance by 5–15% near the stratopause and by up to 20% at the lower altitudes, a reasonably good agreement with the observed profile, which has a 14% rss uncertainty [*Harries et al.*, 1996]. Comparison of Plates 6a and 4c shows that when the model is constrained with the measured profile of H_2O, the ozone deficit does not change appreciably.

However, the abundance of OH, which is a significant sink of ozone in the upper stratosphere and lower mesosphere, is also determined by the partitioning of the HO_x family. In particular, *Clancy et al.* [1994] have shown that their measured concentration of HO_2 between 50 and 70 km is substantially greater than that predicted by the standard chemistry. Underprediction of $[HO_2]$ would likely imply overprediction of [OH] through the reaction, $HO_2 + O \rightarrow OH + O_2$. (That the standard chemistry substantially

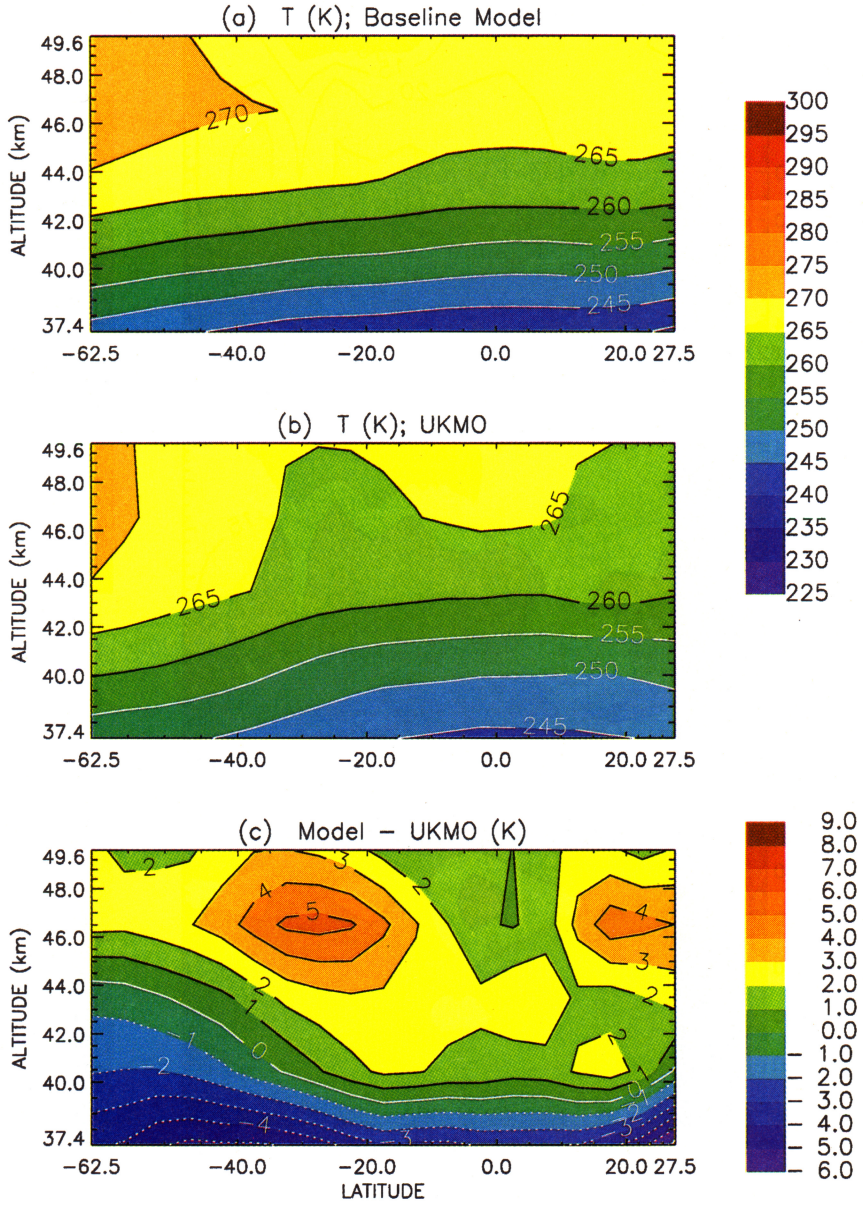

Plate 2. Comparison of (a) the baseline model temperature profile with (b) U.K. Meteorological Office (UKMO) measurements. Both profiles are zonally averaged, and both are for February 13, 1992. (c) The difference shown as model-UKMO. The dotted contours represent cooler model temperatures.

overestimates OH is supported, for example, by the study of *Summers et al.* [1996].) In addition, *Sandor et al.* [1997] have shown that their measurements of molecular oxygen in its first electronically excited state, $O_2(^1\Delta_g)$, between 50 and 70 km are higher than model predictions using JPL94. Since photolysis of ozone is the major source of $O_2(^1\Delta_g)$ in the upper stratosphere and lower mesosphere, they suggest that the ozone deficit is the cause of $O_2(^1\Delta_g)$ underestimation. Further, they show that a 40% reduction in the rate constant of $HO_2 + O \rightarrow OH + O_2$, k_{B2}, uniquely brings model profiles of OH, HO_2, O_3, and $O_2(^1\Delta_g)$ into good agreement with observations.

This 40% reduction is supported in *Sandor's* [1995] comprehensive review of the status of the recommended value of k_{B2} (JPL94), which is the average of values from five experimental studies carried out at room temperature (JPL94, note B2). Excluded from this determination, are the experimental values obtained by *Hack et al.* [1979], because a rate constant they used (k_{B11} for $OH + H_2O_2 \rightarrow H_2O + HO_2$) to derive k_{B2} was in error (JPL94, note B2). However, as pointed out by *Sandor* [1995], when the Hack et al. results are reinterpreted using the correct value for k_{B11}, the resulting k_{B2} agrees with a 40% reduction in the recommended value. This finding, along with the result that the reduced rate constant uniquely resolves the model/data discrepancy discussed above, suggests therefore a need for an experimental evaluation of k_{B2} at stratospheric/mesospheric temperatures to resolve the controversy over its value.

Because of the possibility of a lower k_{B2} discussed above, we conducted an experiment with our model to examine the effect of 40% lower k_{B2} on the ozone abundance. The result is presented in

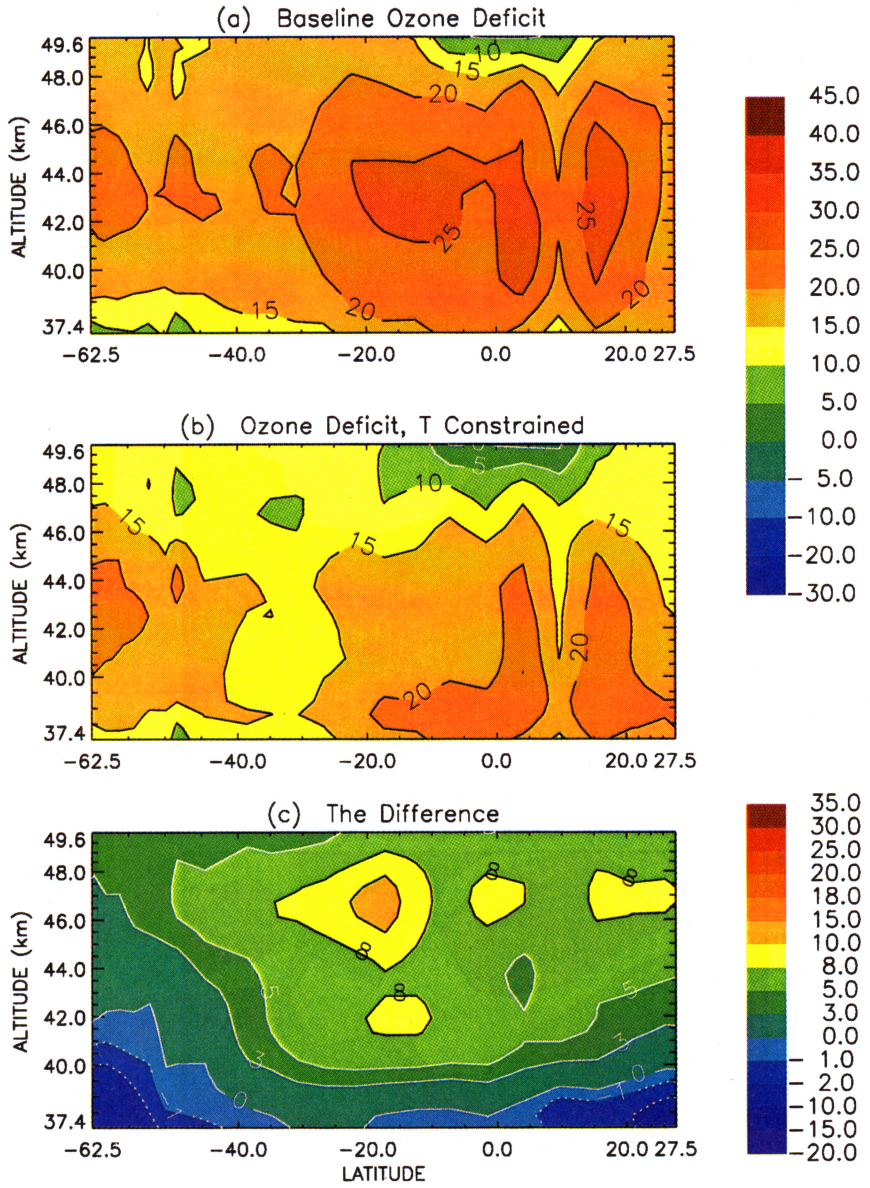

Plate 3. The effect on the ozone deficit due to constraining model temperatures with the observed profile (UKMO): (a) baseline ozone deficit profile for the domain of the study; (b) the ozone deficit when temperature (only) is constrained; and (c) the change (top - middle), the dashed contours showing regions in which the deficit increases (cooler model temperatures than UKMO).

Plate 6b, which shows the ozone deficit profile when T, NO_x, and ClO are constrained and the 40% rate reduction is also applied. It is seen that the ozone deficit is now eliminated, or it is within the rss uncertainties of HALOE O_3 in most of the domain, particularly in the 40 km region. However, near the stratopause the model now overestimates the ozone abundance, although mostly within the observed O_3 uncertainties.

4.1. Comparison With Previous Studies

The results discussed in section 4 are generally consistent with those obtained in many previous investigations of this problem [e.g., *Eluszkiewicz and Allen,* 1993; *Siskind et al.,* 1995] in that our model consistently underestimates the ozone mixing ratio above 35 km. In this respect, however, our results differ from those obtained in the recent study by *Crutzen et al.* [1995]. In particular, the curves for 20°S and 23°S for January 1994 in Figure 1a of that study show an ozone surplus above 40 km. In contrast, the results in the present study for the same latitudes and time of year show an ozone deficit, not only for the baseline case (Plate 3a) but also when the model is constrained with T, NO_x, and ClO (Plate 4c). On the basis of information provided by *Crutzen et al.* [1995], it seems that the reason for obtaining an ozone surplus in their study is the combination of the following: (1) their model was constrained with observed profiles of both HCl and CH_4, which would effectively constrain the [ClO] to almost-observed fields, resulting in reduced ozone loss due to ClO; (2) the NO_x mixing ratios from the version of HALOE data employed [*Crutzen et al.,* 1995] were smaller than those from the version 18 used in the present study; and (3) the corresponding HALOE O_3 mixing

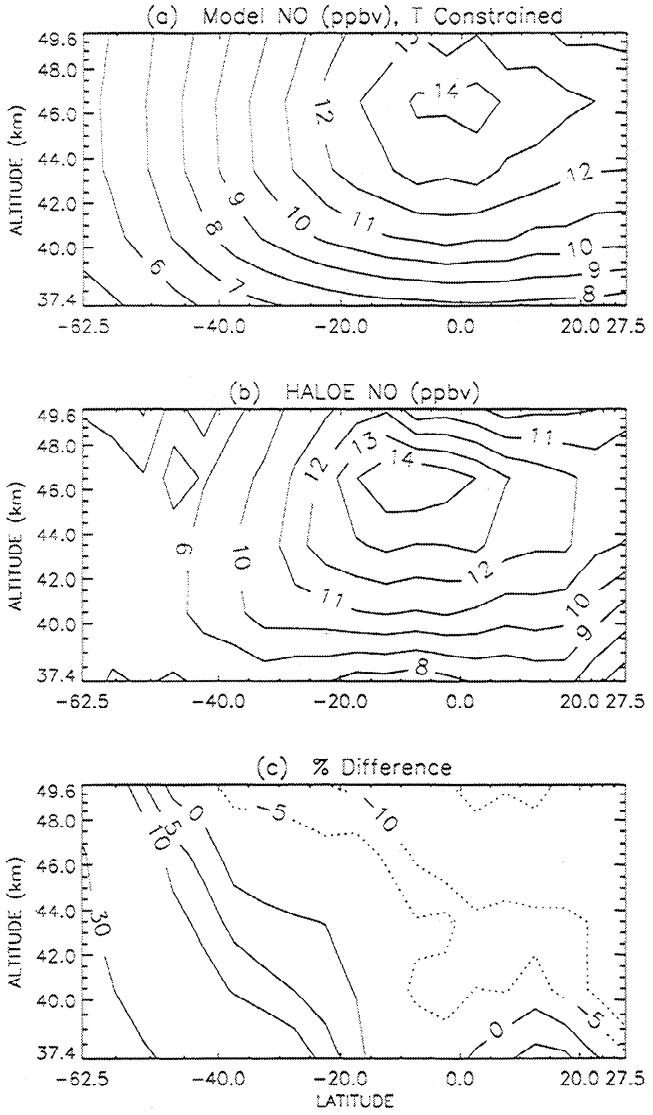

Figure 2. Comparison of NO profile (a) calculated by the model when temperature is constrained with (b) the observed profile from HALOE. Both profiles show sunset zonal means, and are processed for the period of January 6 to February 13, 1992 (section 3.1). (c) The percent difference shown as 100x(HALOE-model)/HALOE. The dotted contours represent overestimation by the model, and the level of the dotted contour at the northern tropical stratopause is -30%.

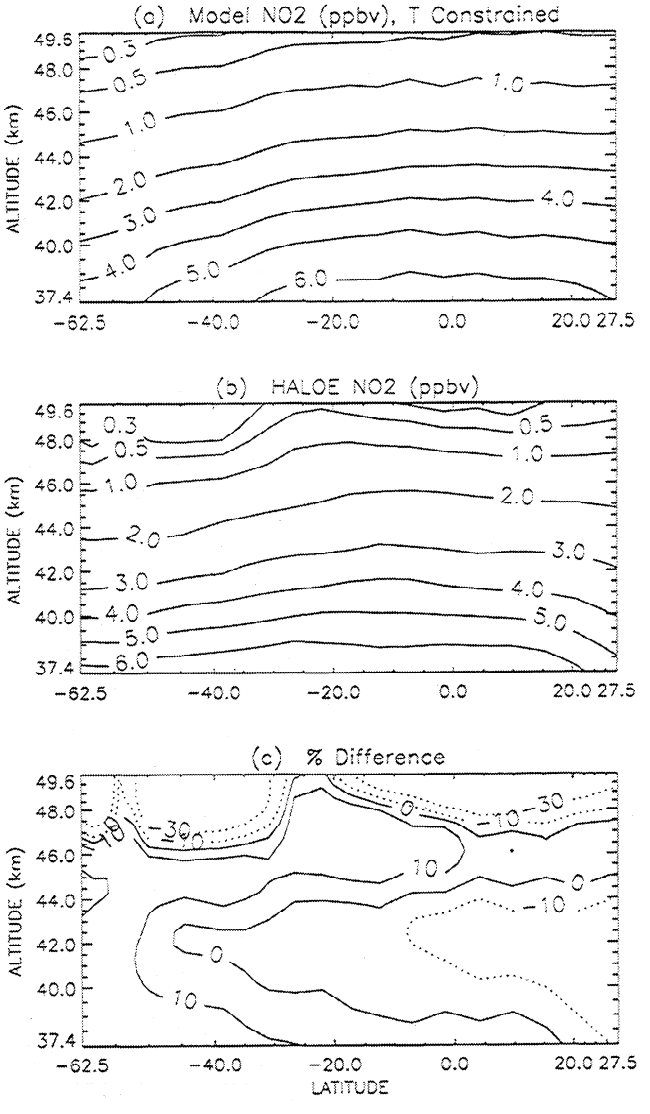

Figure 3. Comparison of NO_2 profile (a) calculated by the model when temperature is constrained with (b) the observed profile from HALOE. Both profiles show sunset zonal means, and are processed for the period of January 6 to February 13, 1992 (section 3.1). (c) The percent difference shown as 100x(HALOE-model)/HALOE. The dotted contours represent overestimation by the model.

ratios were smaller than those from version 18. Moreover, as the results presented here show, the magnitude and sign of the model/data discrepancy in ozone varies with altitude and latitude, so that an apparent lack of deficit at the few latitudes considered in the Crutzen et al. study may not be representative of the situation at other latitudes.

4.2. Possible Solutions for the ClO Overestimation Problem

Since the total chlorine abundance in the model is prescribed (about 3.2 ppbv), the model overestimation of [ClO] implies a potential problem in the calculated partitioning of the Cl_x family. Therefore we compare the model-calculated profile of [ClO]/[HCl], which is a measure of the amount of reactive chlorine to reservoir chlorine, with the corresponding profile derived from observed ClO and HCl distributions (Figure 5). It is seen that the model substantially overestimates this ratio. A species that plays a key role in this partitioning is methane, as seen from the following relationship [*Eluszkiewicz and Allen,* 1993]:

$$\frac{[ClO]}{[HCl]} = \frac{k_{F12}[OH]}{k_{F15}[CH_4] + k_{F38}[HO_2]} \frac{k_{F45}[O_3]}{k_{F1}[O] + k_{F92}[NO]},$$

where the subscripts in the rate coefficients refer to the labels in Table 1 of JPL94, identifying the relevant reactions. Thus an underprediction of $[CH_4]$ by the model would lead to overestimation of [ClO]/[HCl]. We find this to be the case in our

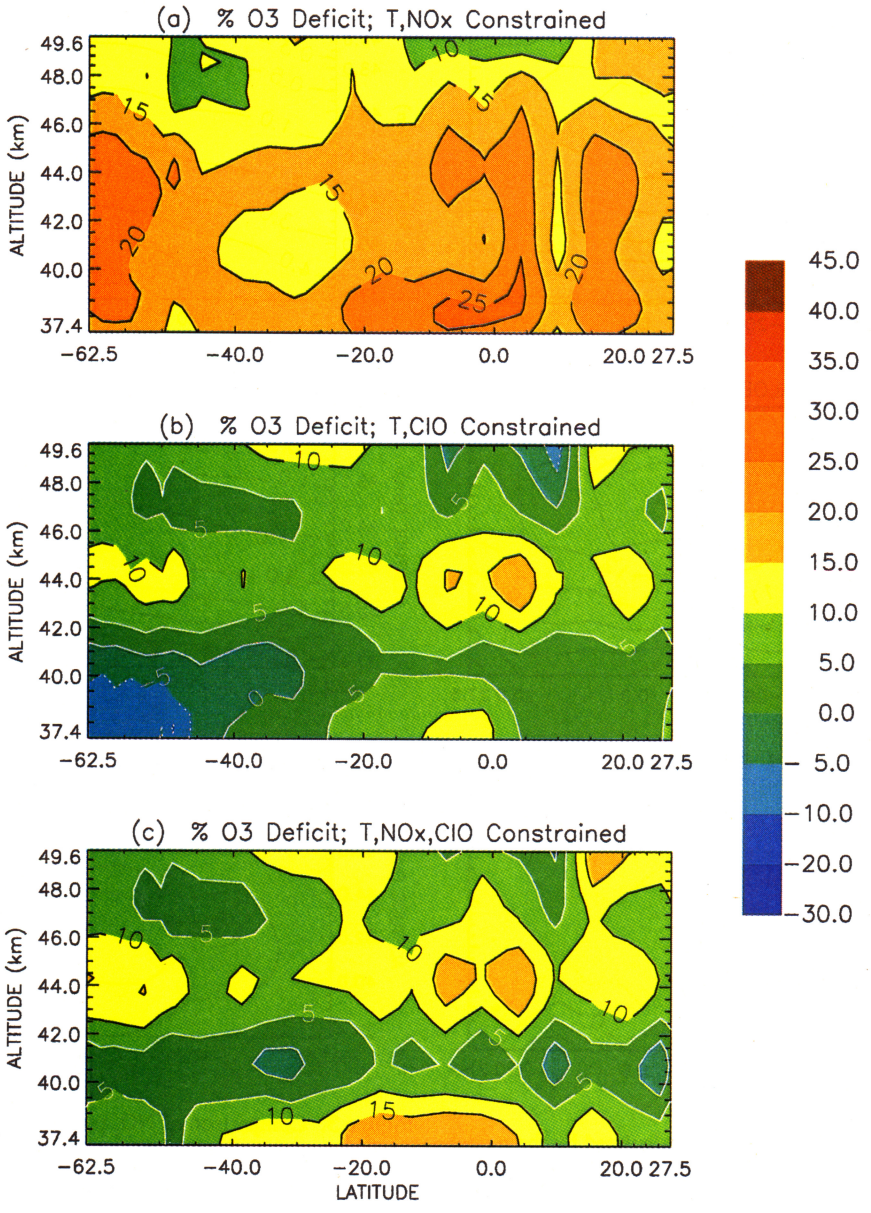

Plate 4. The effect on the ozone deficit profile due to constraining the model with NO_x and ClO: (a) the deficit profile when T and NO_x are constrained; (b) the deficit profile when T and ClO are constrained; and (c) the deficit profile when T, NO_x, and ClO are all constrained.

model. As shown in Figure 6, the methane abundance is underestimated relative to HALOE observations by 10 to 60% in the domain of the study. This model/data discrepancy is mainly due to underestimation in the initial methane profile (provided by our 2-D model) rather than being a characteristic of the standard chemistry, and it has been seen in other studies. For example, as pointed out in section 1.1, *Eluszkiewicz and Allen* [1993] found that the 2-D model of *Yang et al.* [1991] underestimated methane by up to 5 times relative to SAMS measurements. Also, *Solomon and Garcia* [1984] have shown methane underestimation by their 2-D model of up to 2 times at middle to high latitudes in the upper stratosphere, relative to SAMS data.

To examine the effect of CH_4 on ClO, we constrain the model with the observed methane profile (in addition to temperature and NO_x). The ratio of the resulting ClO abundance to that measured by MLS (Plate 5b) is presented in Plate 7a, which shows (compare Plate 5c) that when the model methane profile is in agreement with observation, the overestimation of ClO is significantly reduced but not eliminated.

We address the remaining model/data discrepancy in ClO by first considering the effect of including in the model chemistry the channel of the ClO + OH reaction which leads to the formation of HCl + O_2 (in addition to the standard channel that yields the products Cl + HO_2). This approach has been considered in the

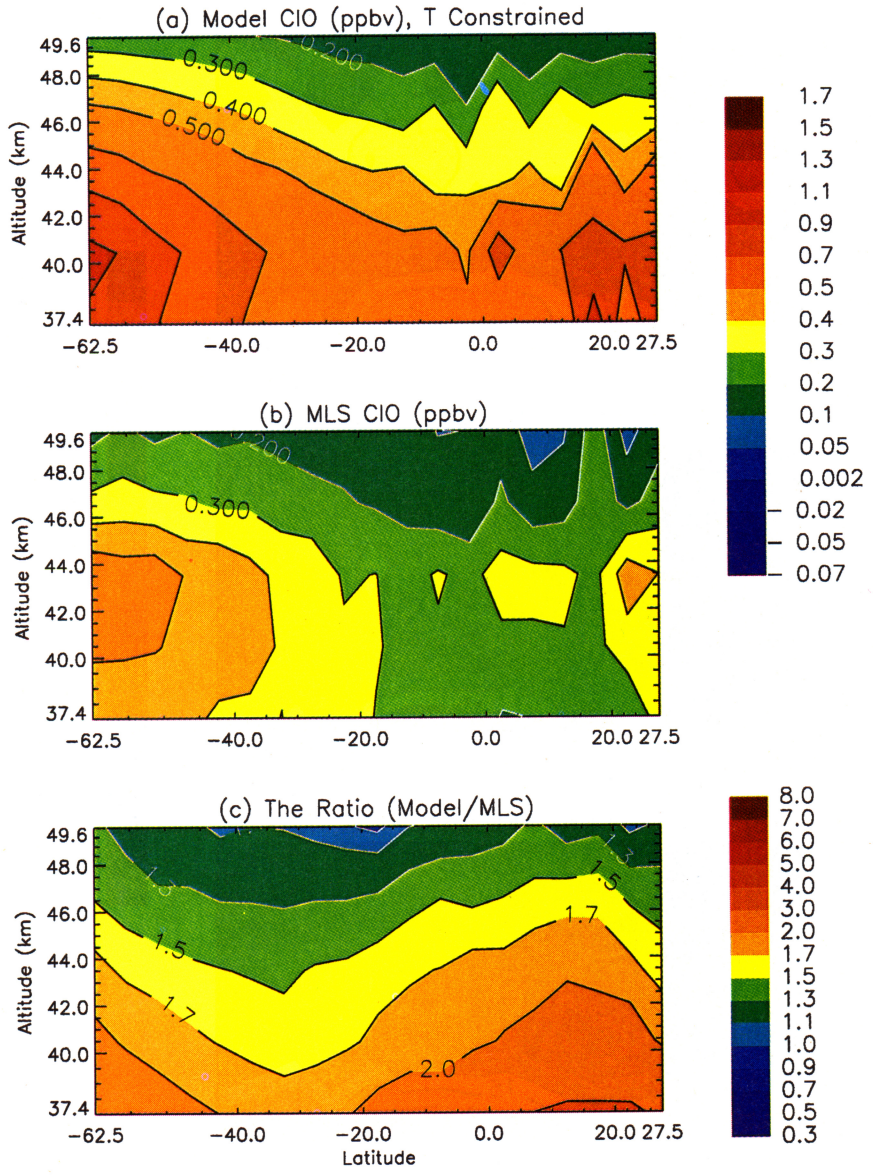

Plate 5. Comparison of the model ClO profile when (a) temperature is constrained, with (b) the profile measured by Microwave Limb Sounder (MLS). Plates 5a and 5b show daytime zonal mean profiles and are processed for the period of January 15 to February 13, 1992 (section 3.2). (c) The ratio (model/observation).

past. For example, *Brasseur et al.* [1985] found that by adding the HCl + O_2 channel with a branching ratio of 15%, the calculated ozone increased by 13% at 40 km. Also, *Toumi and Bekki* [1993], *Chandra et al.* [1993], *Natarajan and Callis* [1991], *Eckman et al.* [1995], and *Michelsen et al.* [1996] concluded that chlorine chemistry is better modeled relative to observations, if this channel is implemented with a branching ratio of 5-10%. In spite of these results, however, the HCl + O_2 branch has not been included in the standard chemistry because of lack of conclusive experimental evidence for the occurrence of HCl as a product [*DeMore et al.*, 1994].

The recent paper by *Lipson et al.* [1997], however, presents laboratory support for this channel with a branching ratio of 0.06±0.02 at 210 K in agreement with the results obtained independently by the kinetics group at National Center for Atmospheric Research (J. Orlando and G. Tyndal, private communication, 1997). Therefore we examine the effect on the calculated ClO profile of including the ClO + OH → HCl + O_2 reaction in our model chemistry. The result is presented in Plate 7b, which shows that when the recommended 6% branching ratio is adopted and when model methane agrees with measurements, the calculated ClO profile is mostly in good agreement with MLS observations.

Next, we investigate the effect on the model ClO abundance of reducing the rate constant of the HO_2 + O → OH + O_2 reaction. As discussed in section 4, a 40% reduction in this rate coefficient

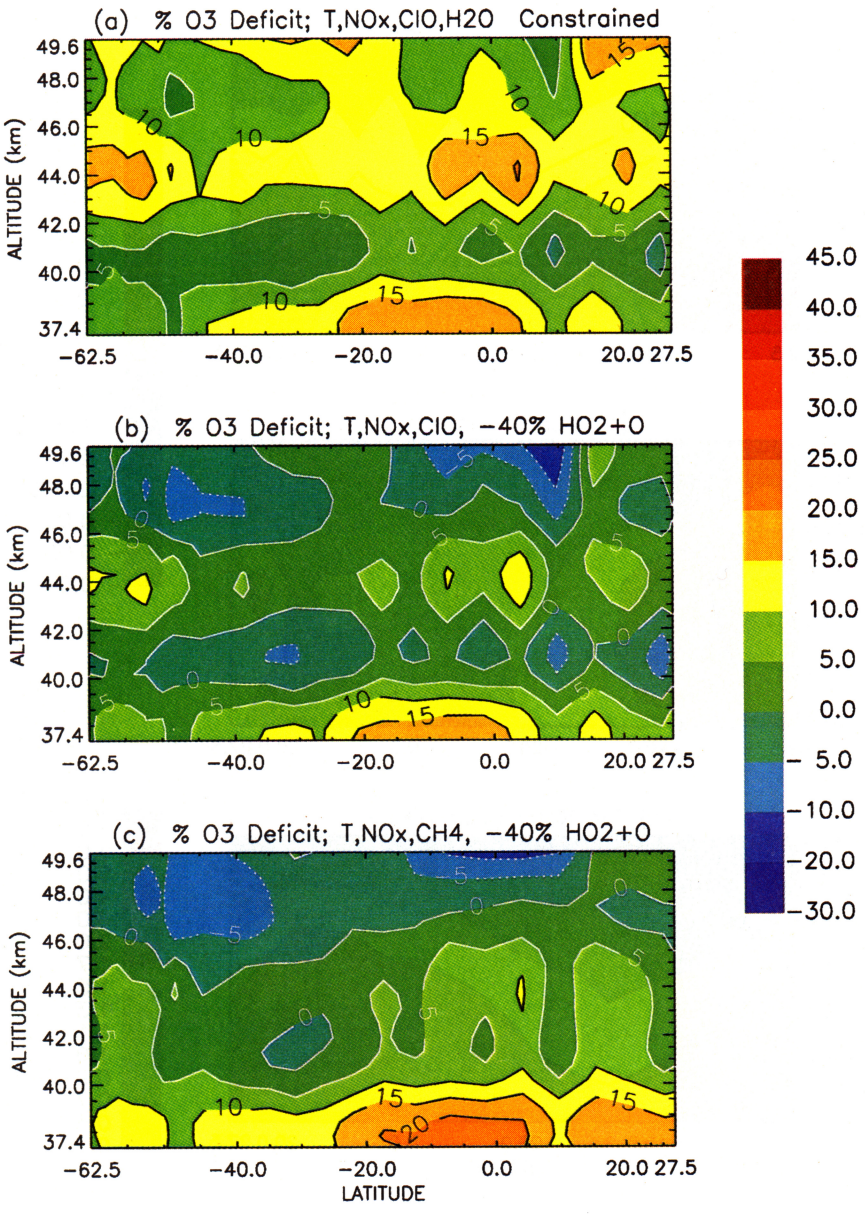

Plate 6. The effect on the ozone deficit profile: (a) due to constraining the model with H_2O, in addition to T, NO_x, and ClO (compare Plate 4c); (b) due to a 40% reduction in the rate constant of $HO_2 + O \rightarrow OH + O_2$ (T, NO_x, and ClO constrained): and (c) due to constraining T, NO_x, and CH_4 and a 40% reduction in the rate constant of $HO_2 + O \rightarrow OH + O_2$.

leads to a decrease in the OH concentration, which decreases the ozone deficit 5 to 10% in the upper altitude range of the study (compare Plates 6b and 4c). Another effect of this reduced [OH] is to lower the concentration of Cl through $HCl + OH \rightarrow Cl + H_2O$, which, in turn, leads to reduced ClO concentrations. This effect is illustrated in Plate 7c, which shows that when the rate constant of $HO_2 + O \rightarrow OH + O_2$ is reduced by 40% (keeping T, NO_x, and CH_4 constrained), the calculated ClO abundance decreases by about 15 to 20% in most of the domain (compare Plate 7a). The corresponding ozone deficit profile is presented in Plate 6c, which shows that in this case the ozone abundance is within the range of HALOE measurement uncertainties except below 40 km where the model still overestimates [ClO] by up to 2 times.

The above results therefore point to two possible mechanisms, which, together with correcting the methane profile (if necessary), would solve the common problem of model overestimation of [ClO] in the upper stratosphere to a large extent. The first mechanism involves the addition of the 6% $HCl + O_2$ channel for the $ClO + OH$ reaction, and the second mechanism involves a decrease in the rate constant of the $HO_2 + O \rightarrow OH + O_2$ reaction (k_{82}). Comparison of Plates 7b and 7c shows that these two mechanisms could yield similar ClO profiles, depending on the magnitude of the rate constant reduction.

Although sensitivity analyses may be carried out to arrive at an "optimal" reduction factor for k_{82}, it would be best to reevaluate this rate constant experimentally (as pointed out in section 4)

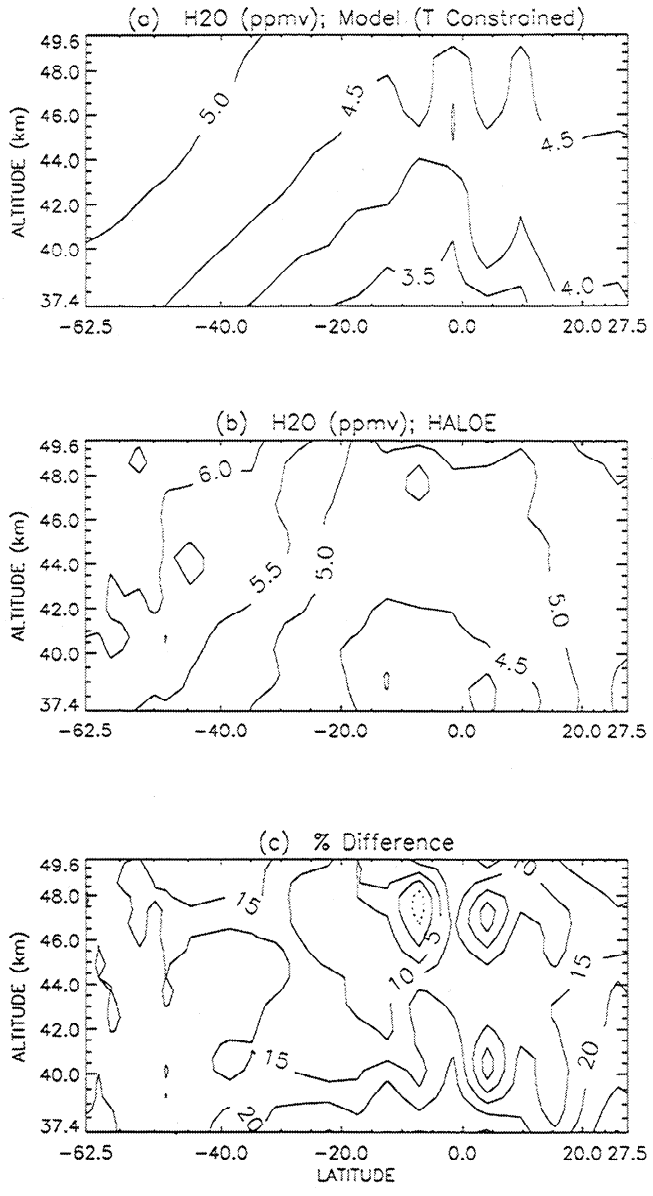

Figure 4. Comparison of H_2O profile (a) calculated by the model when temperature is constrained with (b) the observed profile from HALOE. Both profiles show sunset zonal means, and are processed for the period of January 6 to February 13, 1992 (section 3.1). (c) The percent difference shown as 100x(HALOE-model)/HALOE. The dotted contour represents overestimation by the model.

before drawing any conclusions. Should such a study find that this rate constant is, indeed, lower than the currently recommended value (JPL94), a more comprehensive solution to the ClO problem would be to incorporate into the model chemistry both the reduced rate constant and the HCl + O_2 channel for the ClO + OH reaction.

5. Summary and Conclusions

We have presented a near-global analysis of the ozone deficit problem by constraining a fully diurnal, three-dimensional chemical transport model, with colocated (UARS) measurements of NO, NO_2, ClO, CH_4, H_2O, and O_3, as well as UKMO temperatures. The domain of the study, dictated by the characteristics of the ClO and NO_2 data sets, covers a wide range of altitudes (37.4–49.6 km) and latitudes (62.5°S–27.5°N) for the period of January–February 1992. The baseline model (no constraints) ozone deficit is about 15% at the lower altitudes of the

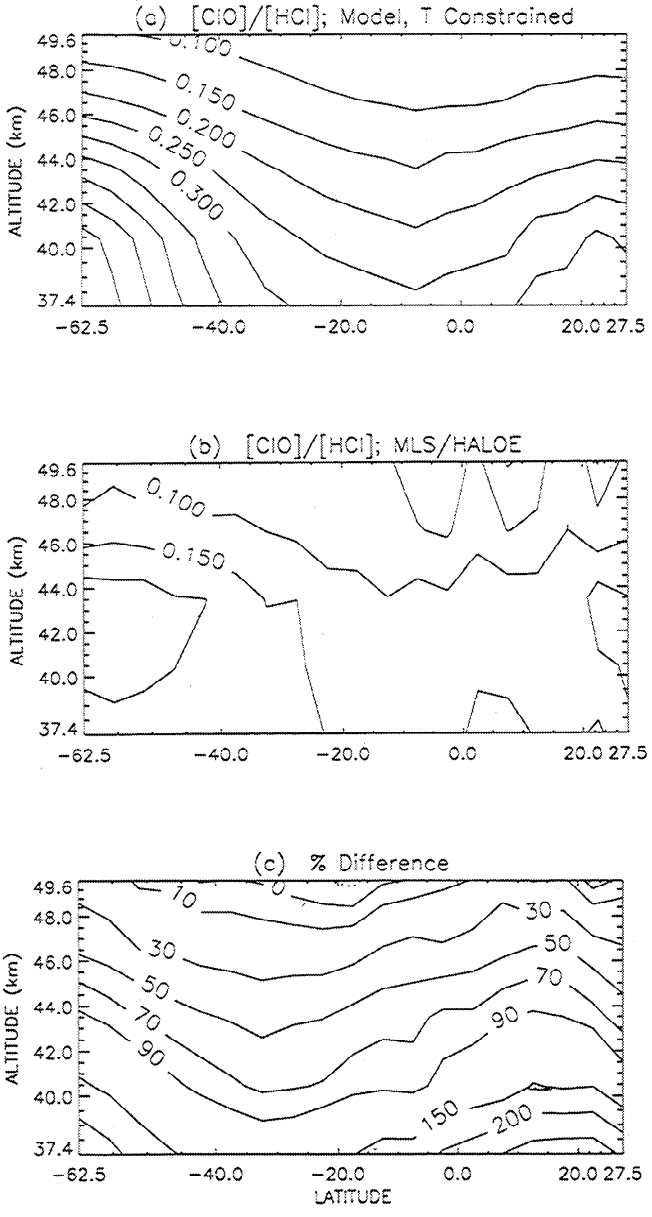

Figure 5. Comparison of (a) the model profile of [ClO]/[HCl], with (b) the observed profile. The observed profile is the ratio of MLS daytime zonal mean ClO to HALOE sunset zonal mean HCl. The same zonal averaging for ClO and HCl (sections 3.1 and 3.2) is used to construct the model-calculated profile in Figure 5a. (c) The difference shown as 100x(model-observed)/model. The dotted contours represent overestimation by the model. The contour level increment in Figures 5a and 5b is 0.05.

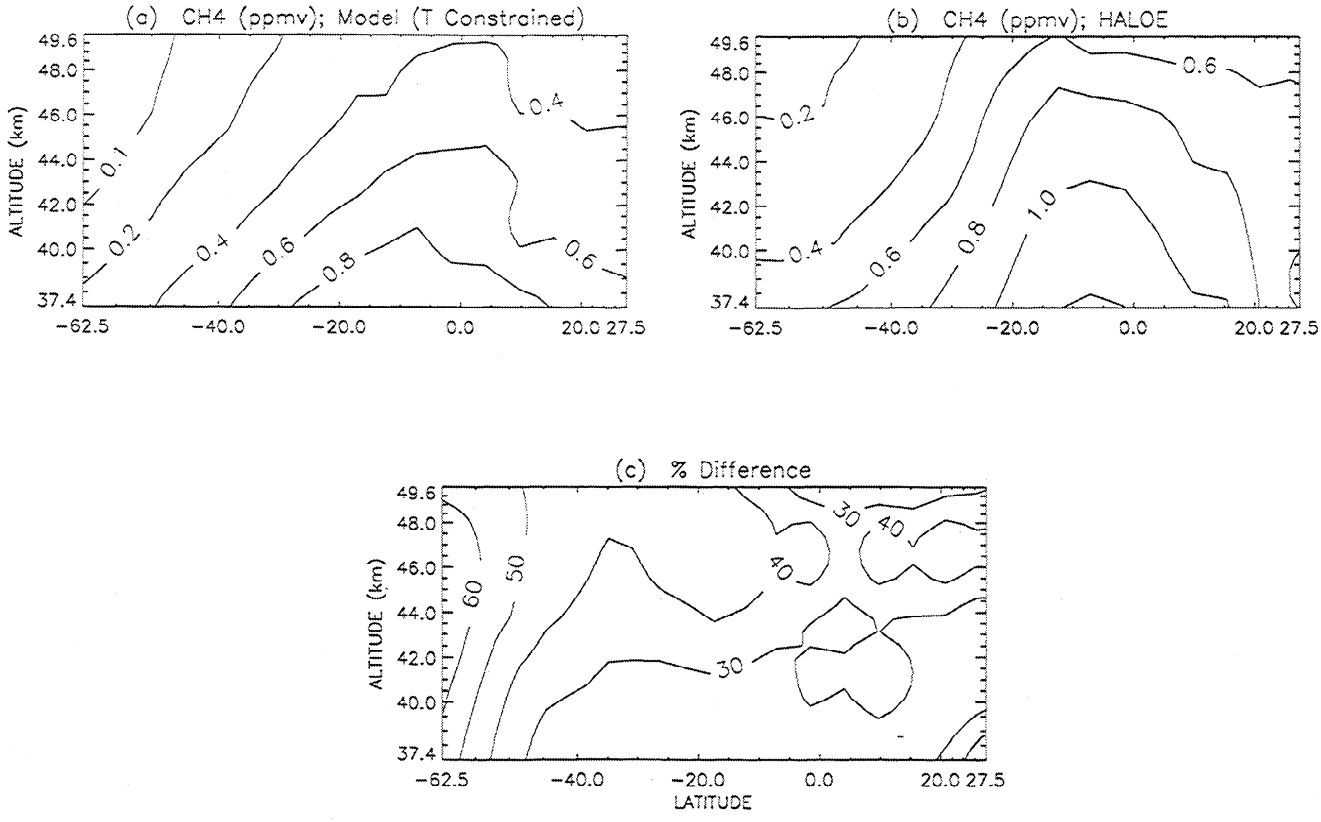

Figure 6. Comparison of CH_4 profile calculated by the model when (a) temperature is constrained, with (b) the observed profile from HALOE. Both profiles show sunset zonal means and are processed for the period of January 6 to February13, 1992 (section 3.1). (c) The percent difference shown as 100x(HALOE-model)/HALOE.

domain, increasing to more than 25% in the 44 km region and decreasing again to 10-15% near the stratopause.

Our results show that in the domain of the study the ozone deficit is decreased by 3-10% when the model temperatures are modified to represent the measurements (UKMO) and that it is further decreased by 5-20% when the model ClO profiles are also adjusted to be in agreement with the observations (MLS). Because the model NO_x and H_2O are generally in good agreement with the HALOE data, constraining the model with the observed NO_x and H_2O profiles leaves the deficit mostly unchanged. When the temperatures and NO_x, H_2O, and ClO concentrations used in the model are all in agreement with measurements, the remaining ozone deficit is about 5-15% in the altitude range of the study (for all latitudes). In particular, the deficit is about 0-5% in the 40 km region, well within the rss uncertainties of the HALOE ozone measurements (8-9%). We also find that by bringing the model methane into agreement with observations and by including a 6% $HCl + O_2$ channel for the ClO + OH reaction, the model ClO profile agrees well with the MLS data in most of the domain.

A similar model/data agreement in [ClO] is obtained when, in addition to constraining the model methane, the rate constant of $HO_2 + O \rightarrow OH + O_2$ is reduced by 40%. This reduced rate constant also eliminates or brings to within HALOE uncertainties the remaining ozone deficit above 38 km. However, in this case the model overestimates the ozone abundance by 5-10% near the equatorial stratopause. These results support the importance of the role of the $HO_2 + O \rightarrow OH + O_2$ reaction in the middle atmospheric chemistry.

Finally, we note that the results of this study regarding the effect of T and ClO on the ozone deficit problem suggest that a significant part of the deficit may not be due to uncertainties in the model input parameters (e.g., rate constants and absorption cross sections). This is because temperature is not an input parameter, and we have shown that the ClO overestimation can be largely eliminated by constraining the methane profile and including the 6% $HCl + O_2$ channel (for the ClO + OH reaction), which has been observed experimentally [*Lipson et al.*, 1997]. Therefore, significant reduction in the upper stratospheric ozone deficit can be obtained over a wide altitude/latitude range (compare Plates 4b and 1c), without adjusting any rate constants or absorption cross sections away from their nominal values given in JPL94.

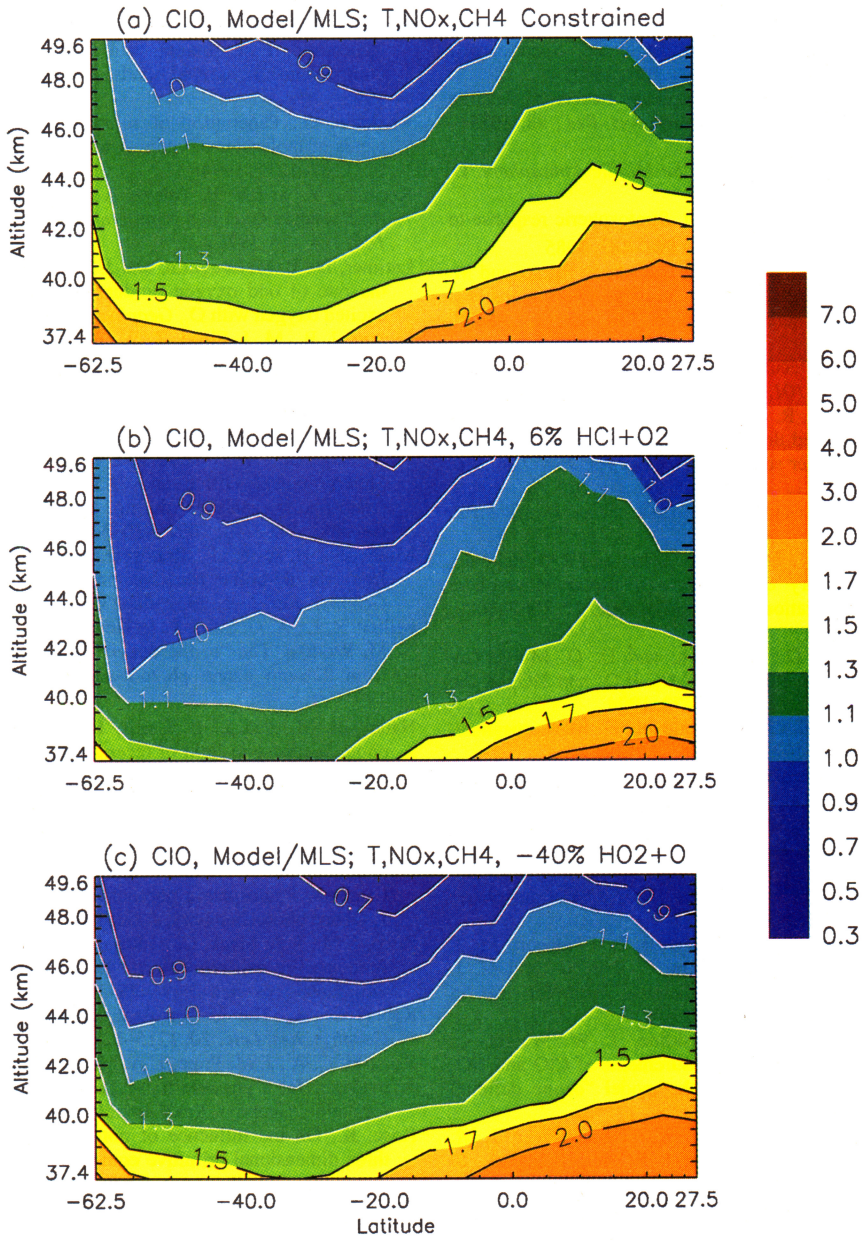

Plate 7. The ratio of model [ClO] to that observed by MLS when in addition to constraining T and NO_x (a) CH_4 is constrained, (b) CH_4 is constrained and a 6% HCl + O_2 branch of ClO + OH is included in the chemistry, and (c) CH_4 is constrained and the rate constant of $HO_2 + O \rightarrow OH + O_2$ is reduced by 40%.

Acknowledgments. We wish to thank Xun Zhu (APL, Johns Hopkins University) for providing his IR radiation code and the relevant input files, William Randel (NCAR) for providing climatological geopotential data, Ken Stone (HALOE group at NASA) for helpful and timely comments on various aspects of the HALOE data sets, Theresa Huang (NCAR) for timely help with evaluating and updating the model's photolysis rates, and Mike Callan (LASP, University of Colorado) for help with IDL programming. This work was mainly supported by a UARS "Guest Investigator" project, NASA grant S-12896-F. The National Center for Atmospheric Research is operated by the University Corporation for Atmospheric Research under sponsorship of the National Science Foundation.

References

Allen, M., A new source of ozone in the terrestrial upper atmosphere?, *J. Geophys. Res., 91*, 2844–2848, 1986.

Allen, M., and M. L. Delitsky, A test of odd oxygen photochemistry using Spacelab 3 Atmospheric Trace Molecule Spectroscopy Observations, *J. Geophys. Res., 96*, 12883–12891, 1991.

Barath, F. T., et al., The Upper Atmosphere Research Satellite Microwave Limb Sounder instrument, *J. Geophys. Res., 98*, 10751–10762, 1993.

Brasseur, G., and S. Solomon, *Aeronomy of the Middle Atmosphere*, D. Reidel, Norwell, Mass., 1986.

Brasseur, G. P., A. De Rudder, and C. Tricot, Stratospheric response to chemical perturbations, *J. Atmos. Chem., 3*, 261–288, 1985.

Brasseur, G., M. H. Hitchman, S. Walters, M. Dymek, E. Falise, and M. Pirre, An interactive chemical dynamical radiative two-dimensional model of the middle atmosphere, *J. Geophys. Res., 95*, 5639–5655, 1990.

Brühl, C., et al., Halogen Occultation Experiment ozone channel validation, *J. Geophys. Res., 101*, 10217–10240, 1996.

Chandra, S., C. H. Jackman, A. R. Douglass, E. L. Fleming, and D. B. Considine, Chlorine catalyzed destruction of ozone: Implications for ozone variability in the upper stratosphere, *Geophys. Res. Lett., 20*, 351–354, 1993.

Chapman, S., A theory of upper-atmosphere ozone, *Mem. R. Meteorol. Soc., 3*, 103, 1930.

Clancy, R. T., D. W. Rusch, R. J. Thomas, M. Allen, and R. S. Eckman, Model ozone photochemistry on the basis of Solar Mesosphere Explorer mesospheric observations, *J. Geophys. Res., 92*, 3067–3080, 1987.

Clancy, R. T., B. J. Sandor, D. W. Rusch, and D. O. Muhleman, Microwave observations and modeling of O_3, H_2O, and HO_2 in the mesosphere, *J. Geophys. Res., 99*, 5465–5473, 1994.

Crutzen, P. J., and U. Schmailzl, Chemical budgets of the stratosphere, *Planet. Space Sci., 31*, 1009–1032, 1983.

Crutzen, P. J., J.-U. Grooss, C. Brühl, R. Müller, and J. M. Russell III, A reevaluation of the ozone budget with HALOE UARS data: No Evidence for the ozone deficit, *Science, 268*, 705–708, 1995.

DeMore, W. B., M. J. Molina, R. T. Watson, D. M. Golden, R. F. Hampson, M. J. Kurylo, C. J. Howard, and A. R. Ravishankara, Chemical kinetics and photochemical data for use in stratospheric modeling, *JPL Publ., 83-62*, 1983.

DeMore, W. B., S. P. Sander, D. M. Golden, R. F. Hampson, M. J. Kurylo, C. J. Howard, A. R. Ravishankara, C. E. Kolb, and M. J. Molina, Chemical kinetics and photochemical data for use in stratospheric modeling, *JPL Publ., 94-26*, 1994.

Dessler, A. E., S. R. Kawa, D. B. Considine, J. W. Waters, L. Froidevaux, and J. B. Kumer, UARS measurements of ClO and NO_2 at 40 and 46 km and implications for the model "ozone deficit," *Geophys. Res. Lett., 23*, 339–342, 1996.

Eckman, R. S., W. L. Grose, R. E. Turner, W. T. Blackshear, J. M. Russell III, L. Froidevaux, J. W. Waters, J. B. Kumer, and A. E. Roche, Stratospheric trace constituents simulated by a three-dimensional general circulation model: Comparison with UARS data, *J. Geophys. Res., 100*, 13951–13966, 1995.

Eluszkiewicz, J., and M. Allen, A global analysis of the ozone deficit in the upper stratosphere and lower mesosphere, *J. Geophys. Res., 98*, 1069–1082, 1993.

Froidevaux, L., M. Allen, and Y. L. Yung, A critical analysis of ClO and O_3 in the midlatitude stratosphere, *J. Geophys. Res., 90*, 12999–13029, 1985.

Froidevaux, L., M. Allen, S. Berman, and A. Daughton, The mean ozone profile and its temperature sensitivity in the upper stratosphere and lower mesosphere: An analysis of LIMS observations, *J. Geophys. Res., 94*, 6389–6417, 1989.

Goody, R. M., and Y. L. Yung, *Atmospheric Radiation*, Oxford Univ. Press, New York, 1989.

Hack, W., A. W. Preuss, F. Temps, and H. G. Wagner, The reaction O + HO_2 → OH + O_2 studied with a LMR-ESR-spectrometer, *Ber. Bunsen Ges. Phys. Chem., 83*, 1275–1279, 1979.

Harries, J. E., J. M. Russell III, A. F. Tuck, L. L. Gordley, P. Purcell, K. Stone, R. M. Bevilacqua, M. Gunson, G. Nedoluha, and W. A. Traub, Validation of measurements of water vapor from the Halogen Occultation Experiment (HALOE), *J. Geophys. Res., 101*, 10205–10216, 1996.

Jackman, C. H., R. S. Stolarski, and J. A. Kaye, Two-dimensional monthly average ozone balance from Limb Infrared Monitor of the Stratosphere and Stratospheric and Mesospheric Sounder data, *J. Geophys. Res.*, 91, 1103–1116, 1986.

Jackman, C. H., E. L. Fleming, S. Chandra, D. B. Considine, and J. E. Rosenfield, Past, present, and future modeled ozone trends with comparisons to observed trends, *J. Geophys. Res., 101*, 28753–28767, 1996.

Kockarts, G., Penetration of solar radiation in the Schumann-Runge bands of molecular oxygen: A robust approximation, *Ann. Geophys., 12*, 1207–1217, 1994.

Kurihara, Y., and R. E. Tuleya, A scheme of dynamic initialization of the boundary layer in a primitive equation model, *Mon. Weather Rev., 106*, 114-123, 1978.

Latimer, D., P. McLoughlin, and J. Wiesenfeld, Detailed balance limits the rate of odd oxygen production in the reaction of vibrationally excited oxygen with O_2, *Geophys. Res. Lett., 23*, 1083–1086, 1996.

Lipson, J. B., M. J. Elrod, T. W. Beiderhase, L. T. Molina, and M. J. Molina, Temperature dependence of the rate constant and branching ratio for the OH + ClO reaction, *J. Chem. Soc. Faraday Trans., 93*, 2665, 1997.

Manney, G. L., R. Swinback, S. T. Massie, M. E. Gelman, A. J. Miller, R. Nagatani, A. O'Neill, and R. W. Zurek, Comparison of U.K. Meteorological Office and U.S. National Meteorological Center stratospheric analyses during northern and southern winter, *J. Geophys. Res., 101*, 10311–10334, 1996.

Michelsen, H. A., et al., Stratospheric chlorine partitioning: Constraints from shuttle-borne measurements of [HCl], [$ClNO_3$], and [ClO], *Geophys. Res. Lett., 23*, 2361–2364, 1996.

Miller, R. L., A. G. Suits, P. L. Houston, R. Toumi, J. A. Mack, and A. M. Wodtke, The "ozone deficit" problem: O_2 (X, v ≥ 26) + O (^{3}P) from 226-nm ozone photodissociation, *Science, 265*, 1831–1838, 1994.

Natarajan, M., and L. B. Callis, Examination of stratospheric ozone photochemistry in light of recent data, *Geophys. Res. Lett., 16*, 473–476, 1989.

Natarajan, M., and L. B. Callis, Stratospheric photochemical studies with Atmospheric Trace Molecule Spectroscopy (ATMOS) measurements, *J. Geophys. Res., 96*, 9361–9370, 1991.

Natarajan, M., L. B. Callis, R. E. Boughner, J. M. Russell III, and J. D. Lambeth, Stratospheric photochemical studies using Nimbus 7 data, 1, Ozone photochemistry, *J. Geophys. Res., 91*, 1153–1166, 1986.

Price, J. M., J. A. Mack, C. A. Rogaski, and A. M. Wodtke, Vibrational-state-specific self-relaxation rate constant measurements of highly vibrationally excited O_2 (v = 19-28), *Chem. Phys., 175*, 83–98, 1993.

Reber, C. A., The Upper Atmosphere Research Satellite (UARS), *Geophys. Res. Lett., 20*, 1215–1218, 1993.

Rogaski, C. A., J. M. Price, J. A. Mack, and A. M. Wodtke, Laboratory evidence for a possible non-LTE mechanism of stratospheric ozone formation, *Geophys. Res. Lett., 20*, 2885–2888, 1993.

Rose, K., On the influence of nonlinear wave-wave interactions in a three dimensional primitive equation model for sudden stratospheric warmings, *Contrib. Atmos. Phys., 56*, 14–41, 1983.

Rose, K., and G. Brasseur, A three-dimensional model of chemically active trace species in the middle atmosphere during disturbed winter conditions, *J. Geophys. Res., 94*, 16387–16403, 1989.

Rusch, D. W., and R. S. Eckman, Implications of the comparison of ozone abundances measured by the Solar Mesosphere Explorer to model calculations, *J. Geophys. Res., 90*, 12991–12998, 1985.

Russell, J. M. III, L. L. Gordley, J. H. Park, S. R. Drayson, W. D. Hesketh, R. J. Cicerone, A. F. Tuck, J. E. Frederick, J. E. Harries, and P. J. Crutzen, The halogen occultation experiment, *J. Geophys. Res., 98*, 10777–10797, 1993.

Sandor, B. J., Microwave studies of chemistry of the middle atmosphere, Ph.D. thesis, Univ. of Colo., Boulder, 1995.

Sandor, B. J., R. T. Clancy, D. W. Rusch, C. E. Randall, R. S. Eckman, D. S. Siskind, and D. O. Muhleman, Microwave observations and modeling of $O_2(^1\Delta_g)$ and O_3 diurnal variation in the mesosphere, *J. Geophys. Res., 102*, 9015–9028, 1997.

Schoeberl, M. R., and D. F. Strobel, The zonally averaged circulation of the middle atmosphere, *J. Atmos. Sci., 35*, 577–591, 1978.

Siskind, D. E., B. J. Connor, R. S. Eckman, E. E. Remsberg, J. J. Tsou, and A. Parrish, An intercomparison of model ozone deficits in the upper stratosphere and mesosphere from two data sets, *J. Geophys. Res., 100*, 11191–11201, 1995.

Slanger, T. G., L. E. Jusinski, G. Black, and G. E. Gadd, A new laboratory source of ozone and its potential atmospheric implications, *Science, 241*, 945–950, 1998.

Smith, A. K., Preconditioning for stratospheric sudden warmings:

Sensitivity studies with a numerical model, *J. Atmos. Sci., 49*, 1003–1019, 1992.

Smith, A. K., Numerical simulation of global variations of temperature, ozone, and trace species in the stratosphere, *J. Geophys. Res., 100*, 1253–1269, 1995.

Smolarkiewicz, P. K., and P. J. Rasch, Monotone advection on the sphere: An Eulerian versus semi-Lagrangian approach, *J. Atmos. Sci., 48*, 793–810, 1991.

Solomon, S., and R. R. Garcia, On the distribution of long-lived tracers and chlorine species in the middle atmosphere, *J. Geophys. Res., 89*, 11633–11644, 1984.

Solomon, S., D. W. Rusch, R. J. Thomas, and R. S. Eckman, Comparison of mesospheric ozone abundances measured by the Solar Mesosphere Explorer and model calculations, *Geophys. Res. Lett., 10*, 249-252, 1983.

Summers, M. E., R. R. Conway, D. E. Siskind, R. Bevilacqua, D. F. Strobel, and S. Zasadil, Mesospheric HO_x photochemistry: Constraints from recent satellite measurements of OH and H_2O, *Geophys. Res. Lett., 23*, 2097–2100, 1996.

Toumi, R., and S. Bekki, The importance of the reactions between OH and ClO for stratospheric ozone, *Geophys. Res. Lett., 20*, 2447–2450, 1993.

Waters, J. W., Microwave limb sounding, in *Atmospheric Remote Sensing by Microwave Radiometry*, edited by M. A. Janssen, chap. 8, pp. 383–496, John Wiley, New York, 1993.

Waters, J. W., et al., Validation of UARS Microwave Limb Sounder ClO measurements, *J. Geophys. Res., 101*, 10091–10127, 1996.

World Meteorological Organization (WMO), Scientific assessment of ozone depletion: 1994, *Global Ozone Res. and Monit. Proj., Rep. 37*, Geneva, 1995.

Yang, H., E. Olaguer, and K. K. Tung, Simulation of the present-day atmospheric ozone, odd nitrogen, chlorine and other species using a coupled 2-D model in isentropic coordinates, *J. Atmos. Sci., 48*, 442–471, 1991.

Zhu, X., An accurate and efficient radiation algorithm for middle atmosphere models, *J. Atmos. Sci., 51*, 3593–3614, 1994.

Zhu, X., M. E. Summers, and D. F. Strobel, Calculation of CO_2 15-μm band atmospheric cooling rates by Curtis matrix interpolation of correlated-k coefficients, *J. Geophys. Res., 97*, 12787–12797, 1992.

G. P. Brasseur, R. Khosravi, and A. K. Smith, National Center for Atmospheric Research, P. O. Box 3000, Boulder, CO 80307. (e-mail: rashid@ncar.ucar.edu)

D. W. Rusch, Laboratory for Atmospheric and Space Physics, University of Colorado, Boulder, CO 80309-0392.

J. M. Russell III, Department of Physics, Hampton University, Hampton, VA 23668.

J. W. Waters, Jet Propulsion Laboratory, California Institute of Technology, 4800 Oak Grove Drive, Pasadena, CA 91109-8099.

(Received August 8, 1997; revised March 27, 1998;
accepted March 27, 1998.)